Preprint Title	Design, synthesis and docking study of acyl thiourea derivatives as possible histone deacetylase inhibitors with a novel zinc binding group
Authors	Duraid H. Al-Amily and Mohammed H. Mohammed
Publication Date	20 Aug 2019
Article Type	Full Research Paper
Supporting Information File 1	Supporting Information File 1.pdf; 190.1 KB
Supporting Information File 2	Supporting Information File 2.pdf; 1.4 MB
Supporting Information File 3	Supporting Information File 3.pdf; 1.3 MB
ORCID® iDs	Duraid H. Al-Amily - https://orcid.org/0000-0002-2143-4268

Design, synthesis and docking study of acyl thiourea derivatives as possible histone deacetylase inhibitors with a novel zinc binding group

Duraid H. Al-Amily* and Mohammad H. Mohammad

Address: Pharmaceutical Chemistry Department, College of Pharmacy-University of Baghdad, Baghdad, Iraq.

Email: Duraid H. Al-Amily – colrelated@copharm.uobaghdad.edu.iq

* Corresponding author

Abstract

Histone deacetylase inhibitors with zinc binding groups often exhibit drawbacks like non-selectivity or toxic effects. Thus, there are continuous efforts to modify the currently available inhibitors or to discover new derivatives to overcome these problems. One approach is to synthesize new compounds with novel zinc binding groups.

The present study describes the utilization of acyl thiourea functionality, known to possess the ability to complex with metals, to be a novel zinc binding group incorporated into the designed histone deacetylase inhibitors. *N*-adipoyl monoanilide thiourea (**4**) and *N*-pimeloyl monoanilide thiourea (**5**) have been synthesized and characterized successfully. They showed good cytotoxicity against cancer cells with low cytotoxicity against normal cells. Their binding mode to the active site of histone deacetylases have been studied by docking study.

Keywords

Histone deacetylase inhibitors, acyl thiourea derivatives, zinc binding group, distance from zinc ion, preferential cytotoxicity.

Introduction

Histone deacetylases (HDACs) comprise a class of enzymes that catalyze the deacetylation of the ε-amino groups of lysine residues at the N-termini of histones [1], proteins that act as a core for DNA compaction into nucleosomes that comprise chromatins [2]. The deacetylation process results in the compaction of nucleosomes and subsequently the repression of gene transcription. Many reports demonstrate that HDACs are overexpressed in several types of cancer [3,4]. Therefore, they represent a valuable target for cancer treatment [5].

In mammalian cells, the identified HDACs represent eighteen isoforms and fall into four major classes (I-IV). Class I includes HDAC1, 2, 3, and 8 while class II includes isoforms 4-7, 9 and 10. Isoform 11 represents class IV. These three classes are zinc-dependent in their activity. The remaining seven isoforms are independent on zinc but, rather, depend on the cofactor nicotine adenine dinucleotide for their catalytic activity and comprise class III [1].

The zinc-dependent classes are most commonly investigated and subjected to inhibition studies as an approach for cancer treatment [6]. HDAC2 is a common example since its crystallographic structure is well resolved [7]. Early studies on the binding site revealed that it is shaped as an internal tunnel-like cavity having a length of 11 Å. At the bottom of this cavity, a zinc ion is positioned followed by a 14 Å foot-like pocket [8] (Figure 1). Lysine residues of histone fit into the tunnel so that they could be deacetylated [9,10].

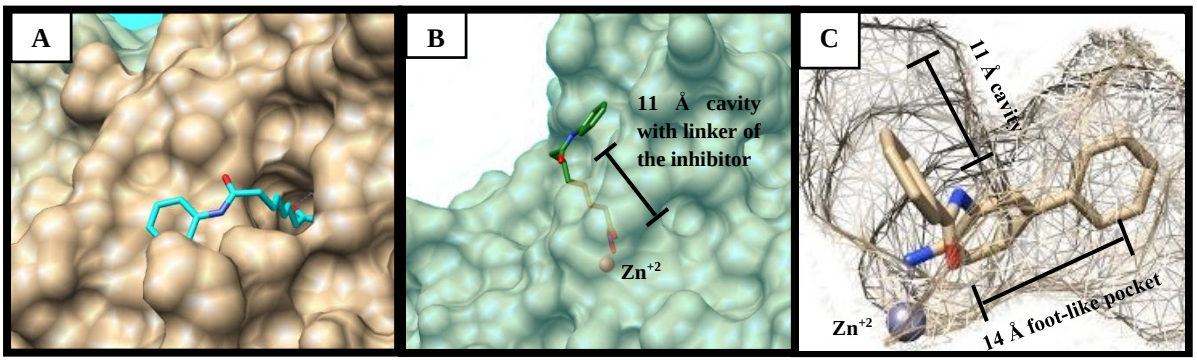

Figure 1: The binding site of HDAC 2. (A): The opening of the tunnel cavity is shown in which the linker of the inhibitor (cyan) is lying. (B): A side view of the binding site with 30% transparency of the surface to make the whole length of the tunnel (11 Å) visible together with

the linker of the inhibitor (forest green). Zinc ion is visible at the deepest end of the tunnel. (C): Mesh surface of the binding site showing the inhibitor inside the 14 Å foot-like pocket.

Accordingly, the design of inhibitors for zinc-dependent HDACs should have a zinc binding group (ZBG) to bind to the zinc ion, a linker chain that mimics acetylated lysine of histone to fit into the cavity, and a hydrophobic cap to recognize and interact with the outer surface. These are best illustrated by the classical, FDA-approved inhibitor suberoylanilide hydroxamic acid **1** (SAHA, vorinostat) [11,12].

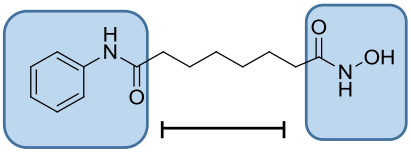

(1)

Other common synthetic inhibitors with ZBG other than hydroxamic acid derivatives include entinostat **2** (MS-275), a benzamide, and the short chain aliphatic carboxylic acid, valproic acid **3** (figure 2)

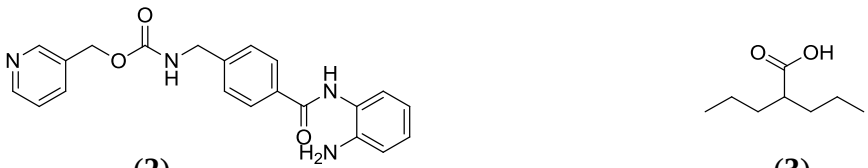

(2) **(3)**

Figure 2: Common HDAIs with ZBG

The most common disadvantages encountered with these classes of inhibitors are related to the poor pharmacokinetic profile and enzyme non-specificity of hydroxamates, *in vivo* toxicity of benzamides due to the free *o*-amine group, and the weak binding of the carboxylic acids to zinc ion [5]. These problems encouraged us to design new compounds that keep both the hydrophobic cap and linker but with a new, unique ZBG.

Acyl thiourea derivatives can coordinate metals in either a bidentate fashion thorough both the carbonyl oxygen and the thiocarbonyl sulfur [13,14], or a monodentate fashion via the

thiocarbonyl sulfur only [15,16] (Figure 3). Thiourea itself can coordinate metals through its sulfur or through one of its nitrogens [17–19].

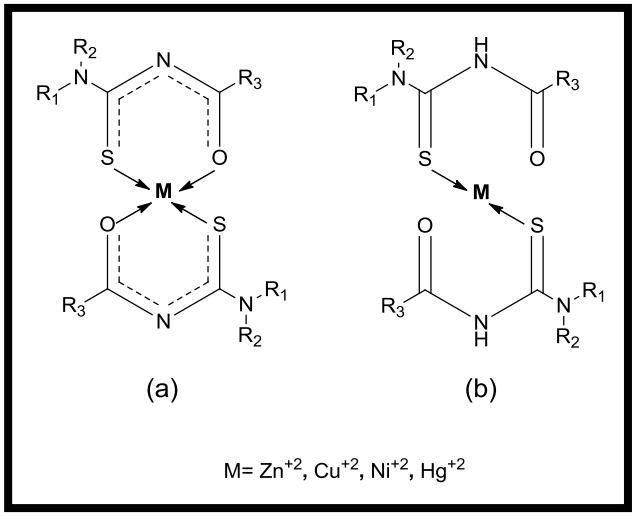

Figure 3: Coordination modes of acyl thiourea derivative with metals as bidentate (a) or monodentate (b)

Here, we wish to describe for the first time the synthesis of two novel substituted acyl thiourea derivatives (compounds **4** and **5**) as possible inhibitors for zinc-dependent histone deacetylase enzymes that have the acyl thiourea as a unique ZBG, a 4- or 5-carbon linker and an aromatic capping group.

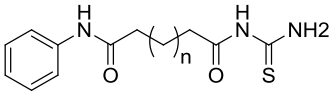

(**4**) n= 2
(**5**) n=3

These compounds have been subjected to docking study against several histone deacetylase enzymes and their binding parameters were compared to those obtained from docking of **1** against the same enzymes. Besides, we will mention the results of the *in vitro* cytotoxicity assay for these compounds against HRT-18 cell line (human colon adenocarcinoma) and HC-04 cell line (mouse hepatoblastoma).

Results and Discussion

Chemical synthesis

Scheme 1 illustrates the synthesis of the target compounds **4** and **5** starting from adipic acid (**4a**) and pimelic acid (**5a**) respectively.

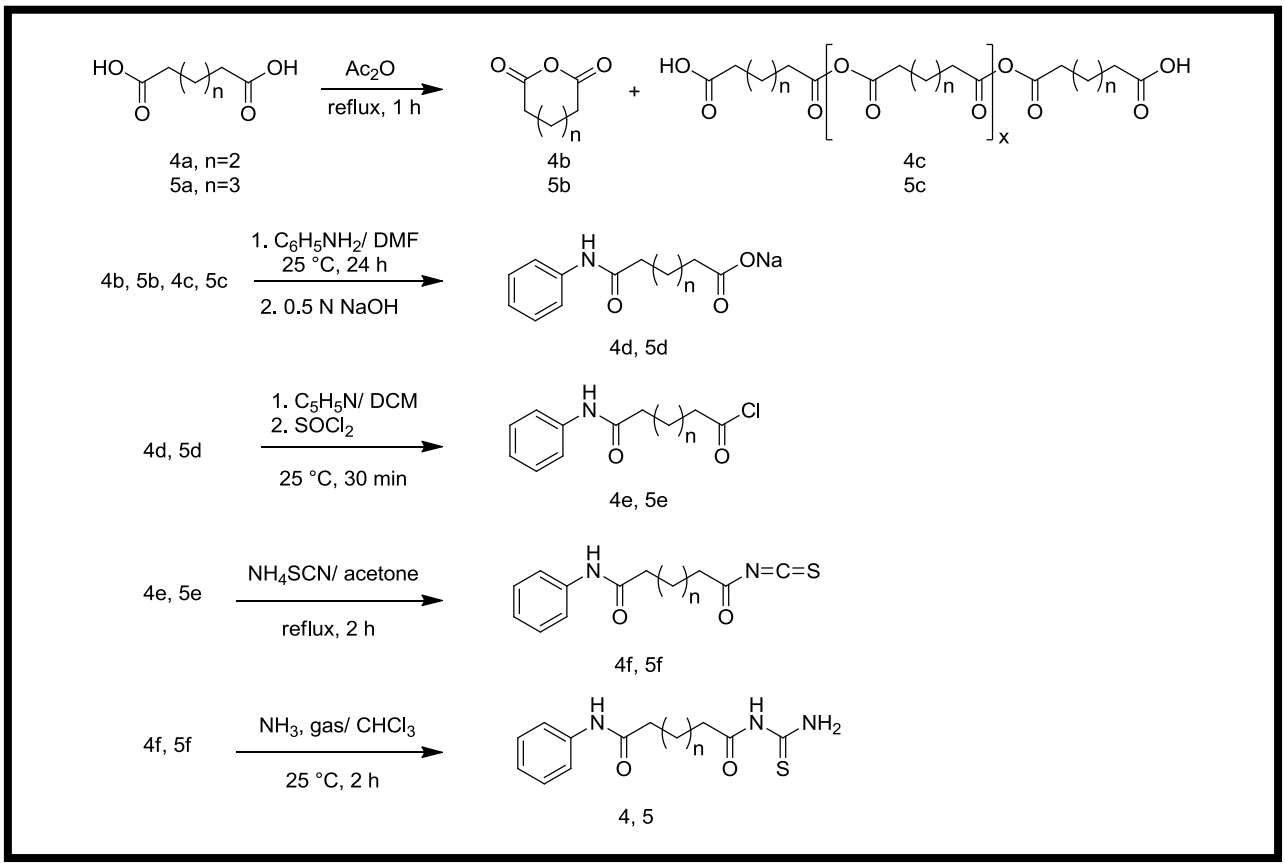

Scheme 1: Synthesis of the target compounds (**4** and **5**)

Synthesis of the target compounds (**4** and **5**) was started from adipic acid and pimelic acid respectively (**4a** and **5a**). Heating these dicarboxylic acids in acetic anhydride for 1 hour would result in monomeric cyclic anhydrides (**4b** and **5b**). However, these anhydrides are extremely instable and some of the synthesized amount is converted into non-cyclic, polymeric anhydrides (**4c** and **5c**) rapidly during evaporation of the solvent [20,21]. The anhydride mixture (**4b**, **5b**, **4c**, and **5c**) was used as such in the next step which is a modified procedure from previously published work [22,23]. In this step, a slight excess of aniline (1.2 eq. relative to **4a** and **5a**) was added gradually to ice-cooled anhydride mixture solution in

dry DMF and then allowed to stir at room temperature for 24 hours. The sodium salts (**4d** and **5d**) were obtained by treatment of the precipitate, resulted after cold acidification of the reaction mixture and filtration, with gradually increasing amounts of ice-cooled NaOH solution (0.5 N) so that the pH was not raised above 7. After filtration and evaporation to dryness, the off white precipitate (**4d** and **5d**) showed the characteristic FT-IR amide peaks (respectively) at 3332 cm^{-1} and 3290 cm^{-1} (aromatic NH) and at 1666 cm^{-1} and 1654 cm^{-1} (amide carbonyl). Furthermore, the carboxylate peaks were at 1562 cm^{-1} (asym. C=O) and 1431 cm^{-1} (sym. C=O) for **4d** and at 1558 cm^{-1} (asym. C=O) and 1435 cm^{-1} (sym. C=O) for **5d**. These anilides were prepared as sodium salts in order to keep the amide function stable during the next step which involved the synthesis of the acid chlorides **4e** and **5e** using thionyl chloride in the presence of 1 equivalent of pyridine [24], thus avoiding the liberation of HCl. Both of the acid chlorides **4e** and **5e** were used directly in the next step, which involved refluxing them with 1 equivalent of ammonium thoicyanate (relative to **4d** and **5d**) in acetone [25,26] for 2 hours to yield the yellow oily isothiocyanates (**4f**, **5f**). These were used directly in the next step, which involved the reaction with gaseous ammonia. This reaction was carried out in a Drechsel gas bottle [27], containing a chloroform solution of **4f** or **5f** and equipped with a stirring bar, by passing a continuous stream of ammonia gas (dried over a column of soda lime). Chloroform was chosen as the reaction solvent since ammonia has a considerable solubility in it through hydrogen bond formation [28]. Unlike a previously published work [26], aqueous ammonia solution was not used to avoid hydrolysis of **4f** and **5f** into the carboxylic acids of monoanilides **4d** and **5d** and thiocyanic acid [29].

The FT-IR spectrum of both of the target acyl thioureas (**4** and **5**, obtained as a yellow precipitate) showed a strong peak at 1149 cm^{-1} that might be attributed to thiocarbonyl (C=S) stretching. They also show two peaks that are attributed to the two amide carbonyls; the peak at 1662 cm^{-1} is attributed to the aromatic amide carbonyl stretching for both of them while the peak at 1705 cm^{-1} (for both) is attributed to the aliphatic amide carbonyl stretching [30–

32]. The latter's unusually high amide carbonyl stretching frequency is probably due to the lone pair of electrons of the thiourea amide nitrogen which lies between two partially positive carbon atoms (carbonyl and thiocarbonyl) since it might spend some of its time at the N–C=S bonds.

The two protons attached to the thiourea primary nitrogen are chemically not equivalent due to the hindered amine rotation [33]. This is illustrated by the difference in their chemical shifts in the ^{1}H-NMR spectrum of **4** and **5** (0.3 ppm and 0.33 ppm respectively). Their peaks (9.34 and 9.64 ppm for **4** and 9.32 and 9.65 ppm for **5**), together with that of thiourea NH (11.06 ppm for **4** and 11.04 ppm for **5**), are of weak intensity since they could be considered as exchangeable protons that usually appear weak or do not appear at all during ^{1}H-NMR spectroscopy using d_6-DMSO as the solvent [34,35].

Cytotoxicity study

Compounds **4** and **5** were tested *in vitro* for antiproliferative activity against HRT-18 cell line (human colon adenocarcinoma), HC-04 cell line (mouse hepatic carcinoma), and HBL-100 cell line (epithelial cells obtained from healthy human breast milk) at micromolar concentrations (6.25, 12.5, 25, 50, 100 µM). Both of them showed inhibitory activity against the cancer cell lines higher than against the normal cell line. Figures 4 and 5 show that there is a continuous and parallel increase in the inhibition of growth exhibited by both compounds against both colon adenocarcinoma and hepatic carcinoma with increasing the concentration. On the other hand, they show very low cytotoxicity against normal cells.

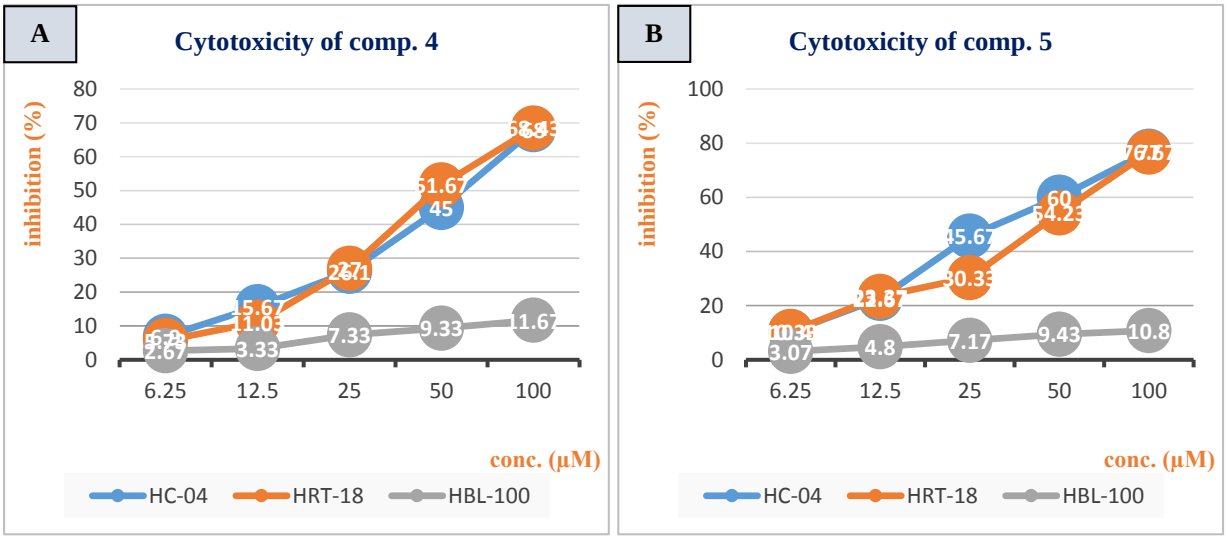

Figure 4: Dose- growth inhibition curve of the tested compounds against hepatic carcinoma cells (blue), colon adenocarcinoma (orange) and healthy breast cells (gray). (A): the cytotoxicity of compound **4**. (B): the cytotoxicity of compound **5**

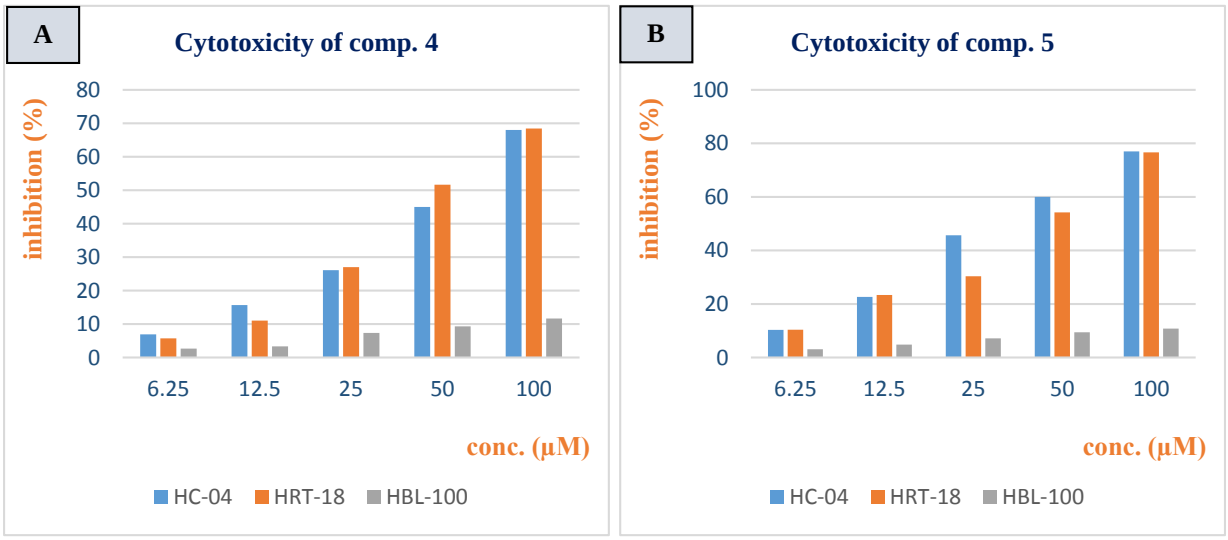

Figure 5: Histogram showing the dose and growth inhibition of the tested compounds against hepatic carcinoma cells (blue), colon adenocarcinoma (orange) and healthy breast cells (gray). (A): the cytotoxicity of compound **4**. (B): the cytotoxicity of compound **5**

Compound **5** was somewhat more cytotoxic than compound **4** against the tested cancer cells. Its IC_{50} against HC-04 cell line and HRT-18 cell line were 21.44 µM and 24.12 µM respectively while those for compound **4** were 27.37 µM and 30.42 µM. Figure 6 (captured at the IC_{50}) shows the difference in magnitude of cytotoxicity between the two compounds.

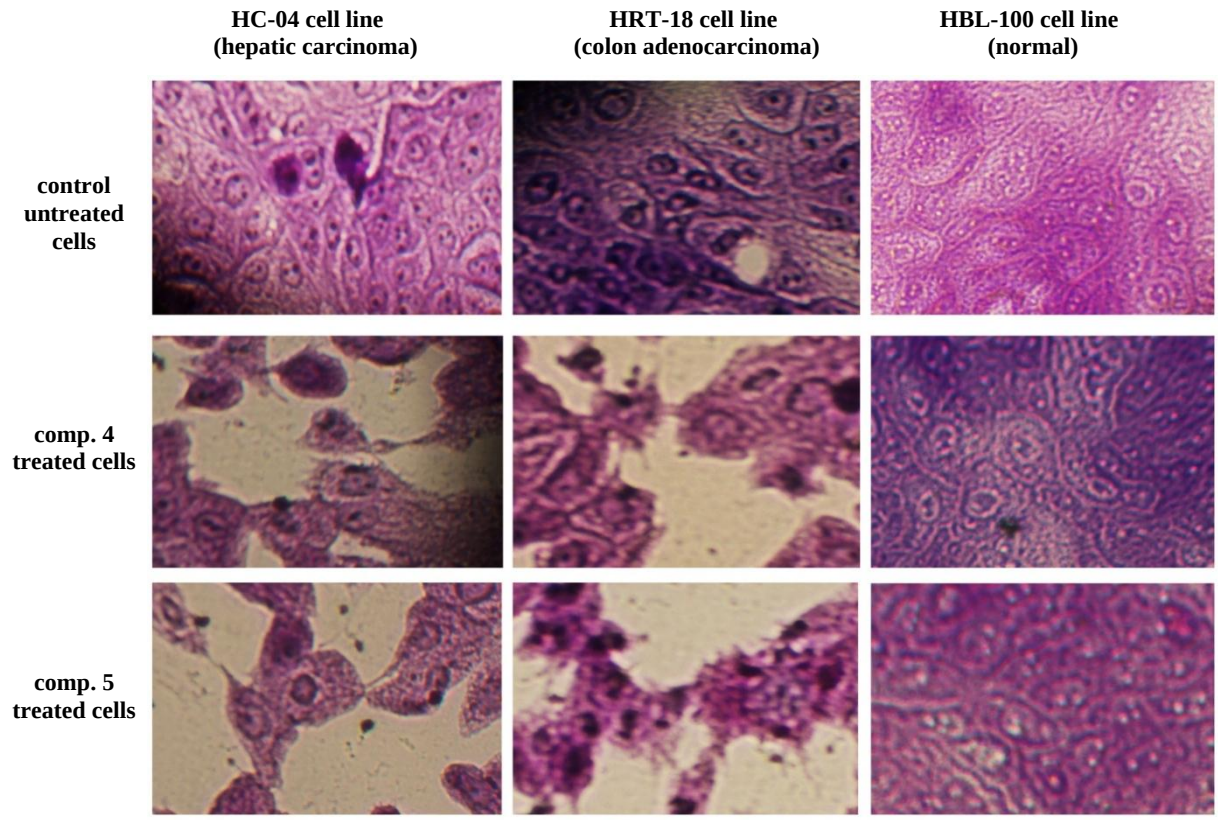

Figure 6: Morphology of the cell lines after treatment with compounds **4** and **5** at the IC_{50} (40x magnified)

Figure 7 illustrates a comparison between the cytotoxicity of these compounds against the tested cell lines.

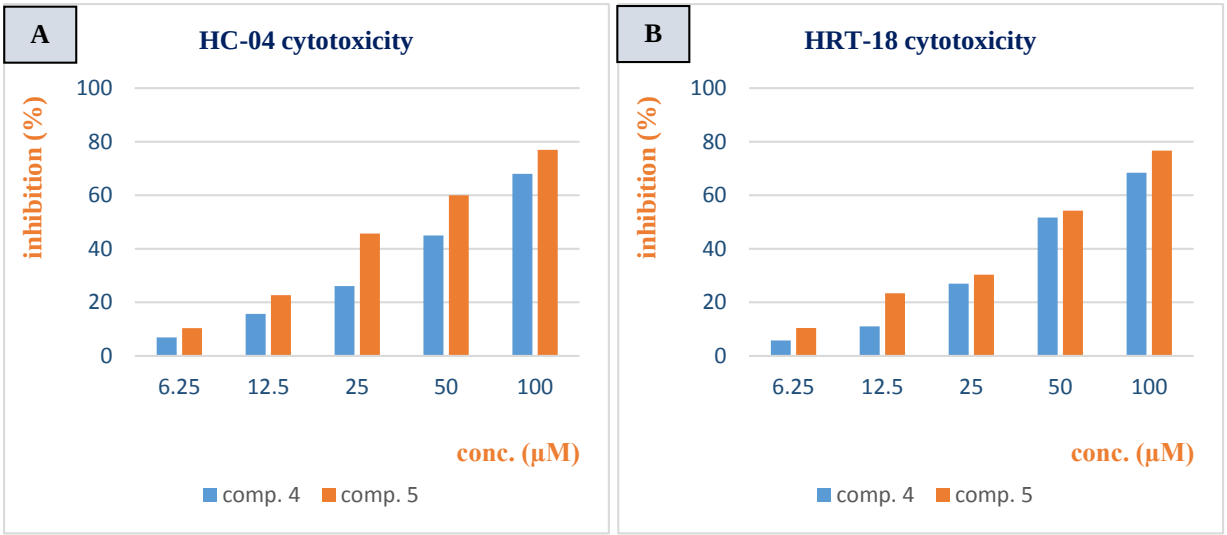

Figure 7: Histogram showing the dose and growth inhibition of the compounds **4** and **5**, (A): against hepatic carcinoma cells and (B): against colon adenocarcinoma

The low cytotoxicity of both compounds against normal cells gives a hope of being able to target cancer cells in a higher degree than normal cells. No more than 12% of

inhibition of growth was observed at the highest concentration used for both compounds (figure 8). This can possibly be considered, in agreement with previous reports [3,4], that the synthesized compounds might exhibit relative specificity in inhibiting HDACs that are overexpressed in cancer cells. Besides, HDAC1 and HDAC2 are absent in normal breast cells [36,37] which further supports this low cytotoxicity in normal tissue, Furthermore, it was hypothesized that normal cells, in contrast to cancer cells, could struggle the inhibitory action of HDAC inhibitors and compensate for the inhibited vital pathways since they have multiple, alternative epigenetic regulatory pathways [38].

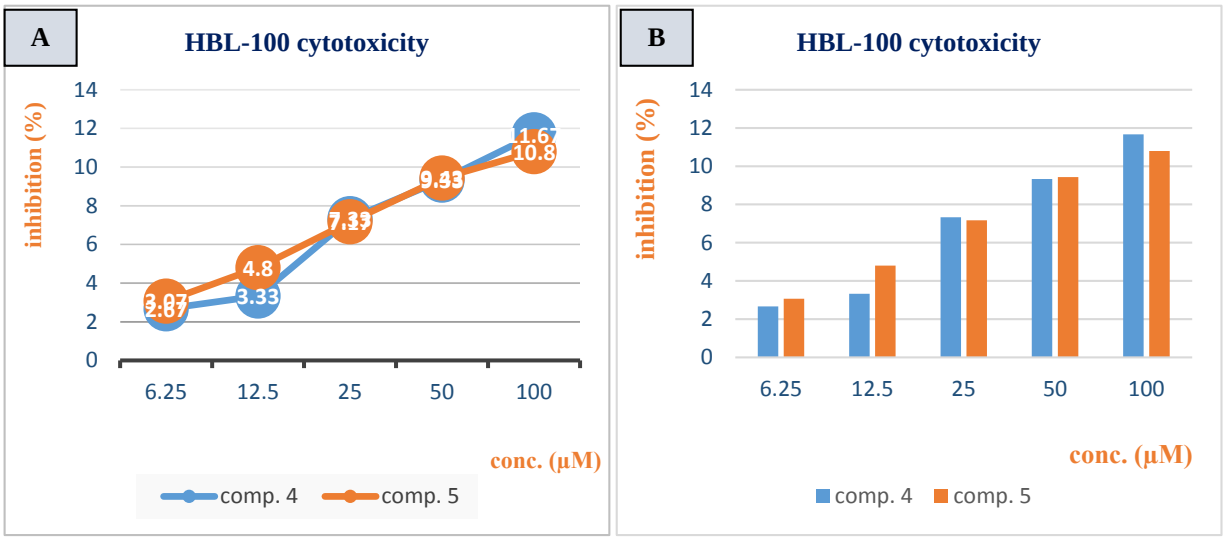

Figure 8: Low cytotoxicity of compounds **4** and **5** on normal breast cells. (A): Dose- growth inhibition curve. (B): Histogram showing the dose and growth inhibition

These findings, besides our docking results, support that our designed and synthesized compounds (**4** and **5**) as being successful HDAC inhibitors.

Docking study

In order to get a preliminary confirmation that compounds **4** and **5** could be successful HDAC inhibitors, their inhibitory mode was simulated by a docking study against several isoforms of HDACs, the crystalline structures of which are confirmed and well resolved and the data of their binding modes to the co-crystallized ligands are available at the protein data bank (PDB, www.rcsb.org) [39].

Compounds **4** and **5** together with SAHA (**1**) (for comparison purposes) were docked against various isoforms of HDACs. These isoforms together with their pdb codes are HDAC1 (5ICN) [40], HDAC2 (4LXZ) [7], HDAC3 (4A69) [41], HDAC4 (5A2S) [42], HDAC7 (3ZNR) [43], HDAC8 (4QA0) [44], and HDAC10 (5TD7) [45].

For each docking, the parameters studied and compared were the binding free energy, the inhibition constant (Ki), number and length of hydrogen bonds between the ligand atoms and amino acid residues located in the binding site of the enzymes, and distance between ligand heteroatoms, which might contribute to zinc binding, and zinc ion of the enzyme.

Since compounds **4** and **5** have been designed to be inhibitors with ZBG, zinc ion was not removed during the enzyme preparation step prior to docking. Moreover, the preparation step included the addition of hydrogen atoms to the enzyme structure to simulate the biological pH (7.4) through correcting the oxidation and tautomeric states of the amino acid residues.

Docking experiments showed that compounds **4** and **5** have binding affinities comparable to, or better than, that of **1** with HDAC2 and HDAC7. Results of docking with these isoforms are summarized in table 1. Images representing the ligand poses as well as hydrogen bond interactions between the ligand and the enzyme are listed in Supporting Information File 3. In order to distinguish the atoms involved in hydrogen bonding, as well as heteroatoms, in the docked compounds, assignment numbers are given to these atoms (figure 9).

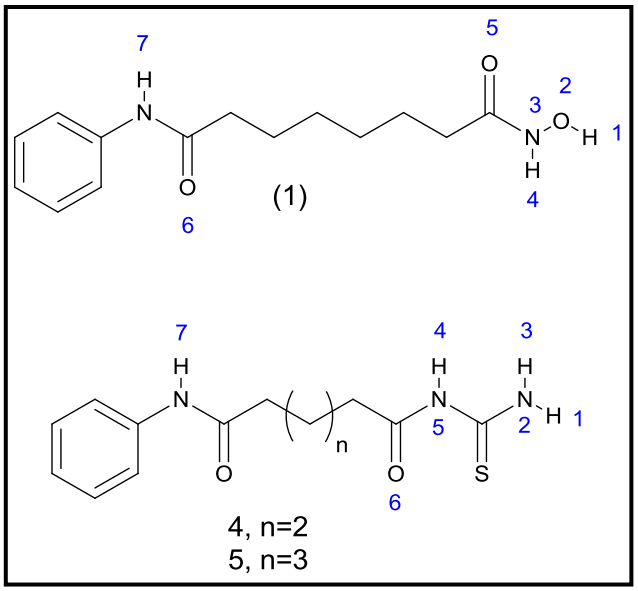

Figure 9: Docked compounds with important atoms assigned number

Table 1: Docking results of compounds **4** and **5** against various HDAC2 and HDAC7

Isoform/ PDB code	Ligand	Pose rank	Energy of binding (Kcal/mol)	K_i	H-bonds				Distance from Zn^{+2} (Å)
					no.	involved ligand atoms	involved residue	length (Å)	
HDAC2/ 4LXZ, chain A	SAHA	1st	-7.1	$6.2*10^{-6}$	1	1H	Tyr297	2.029	2O:5.117 5O:2.198
	4	1st	-7.3	$4.42*10^{-6}$	4	1H	His135	2.3	2N:2.028 S:3.890 6O:4.278
						3H	Asp170(OD1)	2.326	
						3H	Asp170(OD2)	2.165	
						4H	Asp258	2.705	
	5	1st	-7.1	$6.2*10^{-6}$	1	1H	Asp170	2.483	2N:2.012 S:3.889 6O:4.247
HDAC7/ 3ZNR, chain A	SAHA	6th	-6.9	$8.69*10^{-6}$	2	5O	His137	2.311	2O:5.314 5O:2.224
						5O	His136	2.180	
	4	3rd	-7.2	$5.37*10^{-6}$	4	1H	Asp174(OD2)	2.343	2N:1.445 S:3.781 6O:4.819
						1H	Asp174(OD1)	2.204	
						1H	Asp268	2.308	
						6O	His176	2.152	
	5	2nd	-7.2	$5.37*10^{-6}$	3	6O	Gly309	1.986	2N:2.555 S:3.693 6O:4.267
						1H	His176	2.353	
						S	His136	3.176	

The binding energies of compounds **4** and **5** are close to that of **1** when docked to HDAC2, -7.3, -7.1, and -7.1 kcal/mol respectively. Compound **4** has the highest number of hydrogen bonds, four hydrogen bonds. The 5O atom in **1** lies closer to the zinc ion than the 2O atom in. The distance is 2.198 Å between the 5O atom and zinc ion whereas it is 5.117 Å between the 2O atom and zinc ion. The 2N and the S atoms of compounds **4** and **5** show closer distances to the zinc ion than those of **1** atoms; 2.028 Å and 2.012 Å for the 2N atoms of compounds **4** and **5** respectively, and 3.890 Å and 3.889 Å for the S atom of compounds **4** and **5** respectively. This indicates that there is a high possibility for compounds **4** and **5** to coordinate zinc ion [46,47].

Results of docking **1** into HDAC7 showed that it was away from zinc ion in the first five poses. Similarly, **4** was away in the first two poses while **5** was away from zinc ion in the first pose. Accordingly, the binding energy of the sixth pose of **1** with HDAC7 is -6.9 kcal/mol whereas it is -7.2 kcal/mol for both of **4** and **5** (third and second pose respectively). Compounds **1**, **4** and **5** exhibited, respectively, two, four and three hydrogen bonds with amino acid residues located near the end of the binding cavity. The carbonyl oxygen atom (5O) of **1** is 2.224 Å away from zinc ion while the distance between the 2N atom and zinc ion in **4** and **5** is 1.445 Å and 2.555 Å respectively. Furthermore, the S atom of compounds **4** and **5** is closer to the zinc ion than the oxygen atom of the hydroxyl group of **1** (2O); the distances are 3.693 Å and 3.781 Å for compounds **4** and **5** respectively while it is 5.314 Å for **1**.

Results of docking of **4** and **5** into HDAC2 are in agreement with their cytotoxicity results against the chosen cell lines. There is no large difference between the IC_{50} values of both **4** and **5** of the two cancer cell lines (HC-04 and HRT-18), not more than 3 µM (figure 7). This is reflected by the equal binding energies of the two compounds when docked into HDAC2. Likewise, their low cytotoxicity against normal cell lines (figure 8, HBL-100; epithelial cells obtained from healthy human breast milk) is reflected by the exhibited high

affinity when docked into HDAC2 which is, as mentioned above, absent in normal breast cells. All these results collectively indicate that compounds **4** and **5** could be selective HDAC2 inhibitors with their acyl thiourea functionality acting as a novel unique ZBG.

Conclusion

Synthesis of the target acyl thiourea derivatives (**4** and **5**) was achieved successfully starting from adipic acid (**4a**) and pimelic acid (**5a**) respectively. They showed good cytotoxicity against cancer cell lines (HC-04 and HRT-18) and lower cytotoxicity against normal cell line (HBL-100). Their docking study, combined with cytotoxicity results, gave a preliminary indication that they are successful candidates to be HDACIs having the acyl thiourea functionality as a ZBG.

Supporting information

Detailed experimental procedures of chemical synthesis, cytotoxicity study, and docking study are given in Supporting Information File 1. Characterization spectra of the final compounds and intermediates (FT-IR, ^{1}H-NMR and ^{13}C-NMR) are provided in Supporting Information File 2. Figures illustrating poses of the docked ligands into HDAC2 and HDAC7 and their hydrogen bonding are given in Supporting Information File 3.

References

1. Seto, E.; Yoshida, M. Erasers of Histone Acetylation: The Histone Deacetylase Enzymes. *Cold Spring Harb. Perspect. Biol.* **2014**, *6* (4), a018713.
2. Burtis, C. A.; Ashwood, E. R.; Bruns, D. E. *Tietz Textbook of Clinical Chemistry and Molecular Diagnostics*, Fifth.; ELSEVIER: Missouri, 2012.
3. Delcuve, G. P.; Khan, D. H.; Davie, J. R. Targeting Class I Histone Deacetylases in Cancer Therapy. *Expert Opin. Ther. Targets* **2013**, *17* (1), 29–41. https://doi.org/10.1517/14728222.2013.729042.

4. Cao, F.; Zwinderman, M. R. H.; Dekker, F. J. The Process and Strategy for Developing Selective Histone Deacetylase 3 Inhibitors. *Molecules* **2018**, *23*, 551. https://doi.org/10.3390/molecules23030551.

5. Zhang, L.; Zhang, J.; Jiang, Q.; Zhang, L.; Song, W. Zinc Binding Groups for Histone Deacetylase Inhibitors. *J. Enzym. Inhib. Med. Chem.* **2018**, *33* (1), 714–721. https://doi.org/10.1080/14756366.2017.1417274.

6. Kim, H.-J.; Bae, S.-C. Histone Deacetylase Inhibitors: Molecular Mechanisms of Action and Clinical Trials as Anti-Cancer Drugs. *Am. J. Transl. Res.* **2011**, *3* (2), 166–179.

7. Lauffer, B. E. L.; Mintzer, R.; Fong, R.; Mukund, S.; Tam, C.; Zilberleyb, I.; Flicke, B.; Ritscher, A.; Fedorowicz, G.; Vallero, R.; et al. Histone Deacetylase (HDAC) Inhibitor Kinetic Rate Constants Correlate with Cellular Histone Acetylation but Not Transcription and Cell Viability. *j. Biol. Chem.* **2013**, *288* (37), 26926–26943. https://doi.org/10.1074/jbc.M113.490706.

8. Wang, D. F.; Helquist, P.; Wiech, N. L.; Wiest, O. Toward Selective Histone Deacetylase Inhibitor Design: Homology Modeling, Docking Studies, and Molecular Dynamics Simulations of Human Class I Histone Deacetylases. *J. Med. Chem.* **2005**, *48* (22), 6936–6947. https://doi.org/10.1021/jm0505011.

9. Bieliauskas, A. V.; Pflum, M. K. H. Isoform-Selective Histone Deacetylase Inhibitors. *Chem. Soc. Rev.* **2008**, *37* (7), 1402–1413. https://doi.org/10.1039/b703830p.

10. Manal, M.; Chandrasekar, M. J. N.; Gomathi Priya, J.; Nanjan, M. J. Inhibitors of Histone Deacetylase as Antitumor Agents: A Critical Review. *Bioorg. Chem.* **2016**, *67*, 18–42. https://doi.org/10.1016/j.bioorg.2016.05.005.

11. Marks, P. A. Discovery and Development of SAHA as an Anticancer Agent. *Oncogene* **2007**, *26* (9), 1351–1356. https://doi.org/10.1038/sj.onc.1210204.

12. Mann, B. S.; Johnson, J. R.; Cohen, M. H.; Justice, R.; Pazdur, R. FDA Approval Summary: Vorinostat for Treatment of Advanced Primary Cutaneous T-Cell

Lymphoma. *Oncologist* **2007**, *12* (10), 1247–1252. https://doi.org/10.1634/theoncologist.12-10-1247.

13. Binzet, G.; Külcü, N.; Flörke, U.; Arslan, H. Synthesis and Characterization of Cu(II) and Ni(II) Complexes of Some 4-Bromo-N-(Di(Alkyl/Aryl)Carbamothioyl) Benzamide Derivatives. *J. Coord. Chem.* **2009**, *62* (21), 3454–3462. https://doi.org/10.1080/00958970903082200.
14. Saeed, S.; Rashid, N.; Jones, P.; Hussain, R. Thermomechanical Studies of Thermally Stable Metal-Containing Epoxy Polymers from Diglycidyl Ether of Bisphenol A and Amino-Thiourea Metal Complexes. *Eur. J. Chem.* **2011**, *2*, 87–82.
15. Selvakumaran, N.; Sandhiya, L.; Bhuvanesh, N. S. P.; Senthilkumar, K.; Karvembu, R. Structural Diversity in Aroylthiourea Copper Complexes-Formation and Biological Evaluation of [Cu(i)(μ-S)SCl]2,: Cis -Cu(II)S2O2, Trans -Cu(II)S2O2 and Cu(i)S3 Cores. *New J. Chem.* **2016**, *40* (6), 5401–5413. https://doi.org/10.1039/c5nj03536h.
16. Gandhaveeti, R.; Konakanchi, R.; Jyothi, P.; Bhuvanesh, N. S. P.; Anandaram, S. Unusual Coordination Mode of Aroyl/Acyl Thiourea Ligands and Their π-Arene Ruthenium (II) Piano-Stool Complexes: Synthesis, Molecular Geometry, Theoretical Studies and Biological Applications. *Appl. Organometal. Chem.* **2019**, *33* (5), 1–13. https://doi.org/10.1002/aoc.4899.
17. Parmar, S.; Kumar, Y.; Mittal, A. Synthesis, Spectroscopic and Pharmacological Studies of Bivalent Copper, Zinc and Mercury Complexes of Thiourea. *S. Afr. J. Chem.* **2010**, *63*, 123–129.
18. Prakash, J. T. J.; Nirmala, L. R. Synthesis, Spectral and Thermal Properties of Bis Thiourea Zinc Acetate (BTZA) Nonlinear Optical Single Crystal. *Int. J. Comput. Appl.* **2010**, *8* (2), 7–11. https://doi.org/10.5120/1188-1660.
19. Swaminathan, K.; Irving, H. M. N. H. INFRA-RED ABSORPTION SPECTRA COMPLEXES OF THIOUREA. *J. Inorg. Nucl. Chem.* **1964**, *26*, 1291–1294.

20. Herman, D.; Jenssen, K.; Burnett, R.; Soragni, E.; Perlman, S. L.; Gottesfeld, J. M. Histone Deacetylase Inhibitors Reverse Gene Silencing in Friedreich's Ataxia. *Nat. Chem. Biol.* **2006**, *2* (10), 551–558. https://doi.org/10.1038/nchembio815.

21. Julian W. Hill. STUDIES ON POLYMERIZATION AND RING FORMATION. VI. ADIPIC ANHYDRIDE. *J. . Am. Chem. Soc* . **1930**, *52*, 4110–4114.

22. Stowell, J. C.; Huot, R. I.; Van Voast, L. The Synthesis of N-Hydroxy-N′-Phenyloctanediamide and Its Inhibitory Effect on Proliferation of AXC Rat Prostate Cancer Cells. *J. Med. Chem.* **1995**, *38* (8), 1411–1413. https://doi.org/10.1021/jm00008a020.

23. Letton, J. C.; Miller, L. E. Process for the Preparation of Mono-Condensation Derivatives of Adipic Acid. US5286879A, 1994.

24. Wolfe, S.; Godfrey, J. C.; Holdrege, C. T.; Perron, Y. G. Rearrangement of Penicillins to Anhydropenicillins. *Can. J. Chem.* **1968**, *46* (15), 2549–2559.

25. Khairul, W. M.; Daud, A. I.; Mohd Hanifaah, N. A.; Arshad, S.; Razak, I. A.; Zuki, H. M.; Erben, M. F. Structural Study of a Novel Acetylide-Thiourea Derivative and Its Evaluation as a Detector of Benzene. *J. Mol. Struct.* **2017**, *1139*, 353–361. https://doi.org/10.1016/j.molstruc.2017.03.065.

26. Klayman, D. L.; Shine, R. J.; Bower, J. D. The Reaction of S-Methiodide Derivatives of Activated Thioureas with Hydroxylic Compounds. A Novel Synthesis of Mercaptans. *J. Org. Chem.* **1972**, *37*, 1532–1537.

27. Furniss, B. S.; Hannaford, A. J.; Smith, P. W. G.; Tatchell, A. R. *Vogel's Textbook of Practical Organic Chemistry*, Fifth.; Longman Scientific & Technical: England, 1989.

28. Smith, J. F.; Li, C.; Roth, M.; Hepler, L. G. Solubility of Ammonia in Chloroform: Analysis in Terms of Henry's Law and the Equilibrium Constant for Hydrogen-Bonded Complex Formation. *Can. J. Chem.* **1989**, *67* (12), 2213–2217. https://doi.org/10.1139/v89-344.

29. Dixon, E. The Constitution of ‘‘ Thiocyanutes ” Containing a n Electronegativc Group. *J. Chem. Soc., Trans.* **1908**, *93*, 684–700.

30. Wu, J.; Shi, Q.; Chen, Z.; He, M.; Jin, L.; Hu, D. Synthesis and Bioactivity of Pyrazole Acyl Thiourea Derivatives. *Molecules* **2012**, *17* (5), 5139–5150. https://doi.org/10.3390/molecules17055139.

31. Zhong, Z.; Xing, R.; Liu, S.; Wang, L.; Cai, S.; Li, P. Synthesis of Acyl Thiourea Derivatives of Chitosan and Their Antimicrobial Activities in Vitro. *Carbohydr. Res.* **2008**, *343* (3), 566–570. https://doi.org/10.1016/j.carres.2007.11.024.

32. Bai, L.; Li, K.; Li, S.; Wang, J.-X. Phase Transfer Catalytic Synthesis of Phenylacetyl Arylthioureas Under Microwave Irradiation Conditions. *Synth. Commun.* **2002**, *32* (7), 1001–1007. https://doi.org/10.1081/SCC-120003147.

33. Gorobets, N. Y.; Yermolayev, S. A.; Gurley, T.; Gurinov, A. A.; Tolstoy, P. M.; Shenderovich, I. G.; Leadbeater, N. E. Difference between 1H NMR Signals of Primary Amide Protons as a Simple Spectral Index of the Amide Intramolecular Hydrogen Bond Strength. *J. Phys. Org. Chem.* **2012**, *25*, 287–295. https://doi.org/10.1002/poc.1910.

34. Chayah, M.; Camacho, M. E.; Carrión, M. D.; Gallo, M. A. 1 H and 13 C NMR Spectral Assignment of N,N′-Disubstituted Thiourea and Urea Derivatives Active against Nitric Oxide Synthase. *Magn. Reson. Chem.* **2016**, No. January, 793–799. https://doi.org/10.1002/mrc.4455.

35. Firdausiah, S.; S. A Hasbullah; Yamin, B. M. Synthesis , Structurale Elucidation and Antioxidant Study of Ortho- Substituted N , N ’ -Bis (Benzamidothiocarbonyl) Hydrazine Derivatives Synthesis , Structurale Elucidation and Antioxidant Study of Ortho -Substituted N , N ’ -Bis (Benzamidothiocarbon. *J. Phys. Conf. Ser.* **2018**, *979*, 012010.

36. Zhou, H.; Wang, C.; Ye, J.; Chen, H.; Tao, R. Design, Virtual Screening, Molecular Docking and Molecular Dynamics Studies of Novel Urushiol Derivatives as Potential

HDAC2 Selective Inhibitors. *Gene* **2017**, *637* (August), 63–71. https://doi.org/10.1016/j.gene.2017.09.034.

37. RUIJTER, A. J. M. de; GENNIP, A. H. van; CARON, H. N.; KEMP, S.; KUILENBURG, A. B. P. van. Histone Deacetylases (HDACs): Characterization of the Classical HDAC Family. *Biochem. J.* **2003**, *370* (3), 737–749. https://doi.org/10.1042/bj20021321.

38. Eckschlager, T.; Plch, J.; Stiborova, M.; Hrabeta, J. Histone Deacetylase Inhibitors as Anticancer Drugs. *Int. J. Mol. Sci.* **2017**, *18* (7), 1414. https://doi.org/10.3390/ijms18071414.

39. Berman, H. M.; Westbrook, J.; Feng, Z.; Gilliland, G.; Bhat, T. N.; Weissig, H.; Shindyalov, I. N.; Bourne, P. E. The Protein Data Bank. *Nucleic Acids Res.* **2000**, *28* (1), 235–242. https://doi.org/10.1093/nar/28.1.235.

40. Watson, P. J.; Millard, C. J.; Riley, A. M.; Robertson, N. S.; Wright, L. C.; Godage, H. Y.; Cowley, S. M.; Jamieson, A. G.; Potter, B. V. L.; Schwabe, J. W. R. Insights into the Activation Mechanism of Class I HDAC Complexes by Inositol Phosphates. *Nat. Commun.* **2016**, *7*, 11262. https://doi.org/10.1038/pj.2016.37.

41. Watson, P. J.; Fairall, L.; Santos, G. M.; Schwabe, J. W. R. Structure of HDAC3 Bound to Co-Repressor and Inositol Tetraphosphate. *Nature* **2012**, *481* (7381), 335–340. https://doi.org/10.1038/nature10728.

42. Luckhurst, C. A.; Breccia, P.; Stott, A. J.; Aziz, O.; Birch, H. L.; Bürli, R. W.; Hughes, S. J.; Jarvis, R. E.; Lamers, M.; Leonard, P. M.; et al. Potent, Selective, and CNS-Penetrant Tetrasubstituted Cyclopropane Class IIa Histone Deacetylase (HDAC) Inhibitors. *ACS Med. Chem. Lett.* **2016**, *7* (1), 34–39. https://doi.org/10.1021/acsmedchemlett.5b00302.

43. Lobera, M.; Madauss, K. P.; Pohlhaus, D. T.; Wright, Q. G.; Trocha, M.; Schmidt, D. R.; Baloglu, E.; Trump, R. P.; Head, M. S.; Hofmann, G. A.; et al. Selective Class IIa

Histone Deacetylase Inhibition via a Nonchelating Zinc-Binding Group. *Nat. Chem. Biol.* **2013**, *9* (5), 319–325. https://doi.org/10.1038/nchembio.1223.

44. Decroos, C.; Bowman, C. M.; Moser, J. A. S.; Christianson, K. E.; Deardorff, M. A.; Christianson, D. W. Compromised Structure and Function of HDAC8 Mutants Identified in Cornelia de Lange Syndrome Spectrum Disorders. *ACS Chem. Biol.* **2014**, *9* (9), 2157–2164. https://doi.org/10.1021/cb5003762.

45. Hai, Y.; Shinsky, S. A.; Porter, N. J.; Christianson, D. W. Histone Deacetylase 10 Structure and Molecular Function as a Polyamine Deacetylase. *Nat. Commun.* **2017**, *8* (May), 15368. https://doi.org/10.1038/ncomms15368.

46. Jones, P.; Bottomley, M. J.; Carfí, A.; Cecchetti, O.; Ferrigno, F.; Lo Surdo, P.; Ontoria, J. M.; Rowley, M.; Scarpelli, R.; Schultz-Fademrecht, C.; et al. 2-Trifluoroacetylthiophenes, a Novel Series of Potent and Selective Class II Histone Deacetylase Inhibitors. *Bioorg. Med. Chem. Lett.* **2008**, *18* (11), 3456–3461. https://doi.org/10.1016/j.bmcl.2008.02.026.

47. Abdel-Atty, M. M.; Farag, N. A.; Kassab, S. E.; Serya, R. A. T.; Abouzid, K. A. M. Design, Synthesis, 3D Pharmacophore, QSAR, and Docking Studies of Carboxylic Acid Derivatives as Histone Deacetylase Inhibitors and Cytotoxic Agents. *Bioorg. Chem.* **2014**, *57*, 65–82. https://doi.org/10.1016/j.bioorg.2014.08.006.